IPP-Report

Max-Planck-Institut für Plasmaphysik

H. Wobig, E. Harmeyer, F. Herrnegger, J. Kisslinger

The Magnetic Field of Modular Coils

IPP 12/5
December, 2009

The Magnetic Field of Modular Coils

H. Wobig, E. Harmeyer, F. Herrnegger, J. Kisslinger
Max-Planck-Institut für Plasmaphysik, 8046 Garching Fed. Rep. of Germany

January 21, 2009

Abstract

The paper investigates the magnetic field of modular coils in stellarators. Introducing a local coordinate system the magnetic inside the coil and outside the coil is computed. The magnetic field of a coil with rectangular cross section can be reduced to elementary function leaving an one-dimensional integration along the coil axis. Trapezoidal shape of the coil cross section and inhomogeneous current density offer the chance to reduce the maximum field on the boundary of the coil. In this case reduction to elementary functions is not possible. In large distance from the coil the magnetic field can be computed by Biot-Savart's law, however, close to the coils and in the boundary region of magnetic surfaces higher order corrections must be taken into account. A numerical example demonstrates the difference between the various approximations.

1 Introduction

The term modular stellarator refers to a generalized stellarator configuration with nested magnetic surfaces and with multiple helicity achieved by a system of discrete coils which provide both toroidal and poloidal fields [1]. Since there is no net toroidal current, no extra vertical field coils are needed. A modular stellarator has no continuous helical windings; all coils are closed poloidally. Furthermore, there is no force pointing inwards as in case of helical windings and consequently the support structure can be located outside and between the coils.

Modular coils offer the chance to realize a large variety of stellarator configurations, which cannot be achieved by continuous helical coils. In particular, this refers to the superposition of helical fields with different helicity and a toroidal mirror field, which is desirable in the search for optimum configurations. Here optimisations means to shape magnetic surfaces and rotational transform in view of an optimum plasma equilibrium, stability and neoclassical confinement. The following figure (Fig.1) displays a typical example of a modular coil in stellarators. The magnetic field of a coil at a position $\boldsymbol{X}$ is given by

$$\boldsymbol{B} = \nabla \times \boldsymbol{A} \quad ; \quad \boldsymbol{A}(\boldsymbol{X}) = \frac{\mu_0}{4\pi} \int \frac{\boldsymbol{j}(\boldsymbol{x}) d^3\boldsymbol{x}}{|\boldsymbol{X} - \boldsymbol{x}|} \tag{1}$$

In some distance to the coil the Biot-Savart equation may be an acceptable approximation, however, inside the coil the singularity at $\boldsymbol{X} = \boldsymbol{x}$ requires a careful procedure. The EFFI-code [2] approximates the volume integration in eq.(25) by a sum of integrals

$$\boldsymbol{A}(\boldsymbol{X}) = \frac{\mu_0}{4\pi} \int \frac{\boldsymbol{j}(\boldsymbol{x})}{|\boldsymbol{X} - \boldsymbol{x}|}\, d^3\boldsymbol{x} \approx \frac{\mu_0}{4\pi} \sum_k \int \frac{\boldsymbol{j}(\boldsymbol{x})}{|\boldsymbol{X} - \boldsymbol{x}|}\, dV_k \tag{2}$$

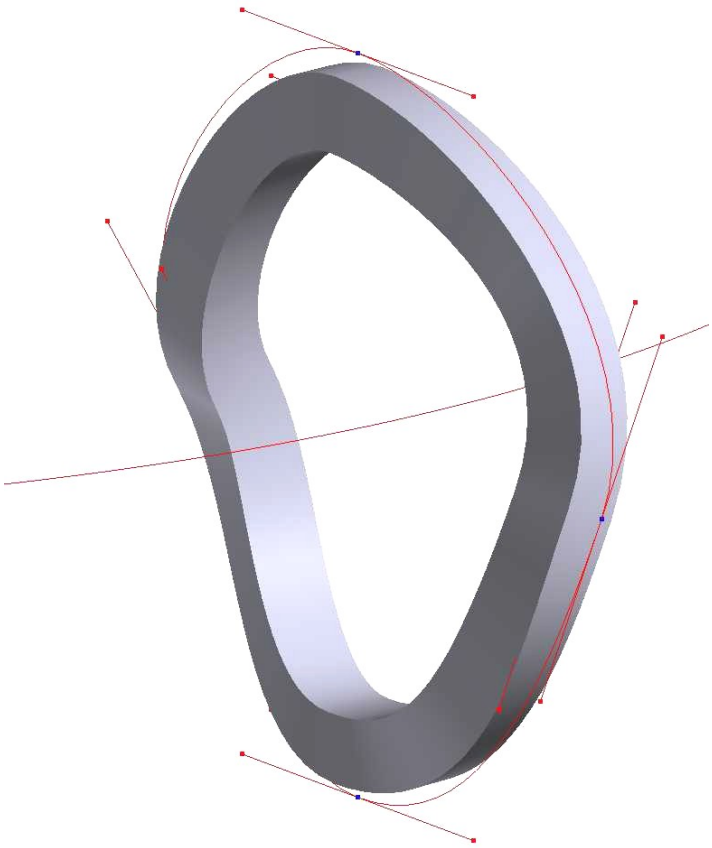

Figure 1: Modular coil of a stellarator. The central filament (not shown in the figure) and the red auxiliary curve define the normal vector and the binormal vector of the coil.

where dV_k are rectangular volume elements. The integration over these volume elements can be performed in terms of elementary functions, however, since a three-dimensional coil cannot be completely covered by rectangular volume elements gaps remain and the computations is not quite correct. Furthermore, as will be shown in the analysis, the EFFI-approximation neglects curvature effects. The magnetic field of circular arcs has been studied extensively by L. Urankar [3], this geometry can also be described by elementary functions. Approximating a modular coil by a set of arcs is faced with the problem of discontinuities at the gaps between arcs. The magnetic field of circular coils has als been computed by M. Fontana [7]. Prismatic segments of coils have been studied by S. Babic and C. Akyel [8], who found analytic expressions for such segments. These solutions are helpful in computing the magnetic field of planar coils which can be approximated by a system of straight segments, arc segments and prismatic segments. Modular coils of stellarators, however, are 3-dimensional, the torsion of the coil introduces a new aspect which cannot be covered by these three elementary segments.

Another procedure is a decomposition of the windig pack in a set of tetrahedral regions. Applying Gauss' theorem reduces the volume integral to surface integrals over the faces and as a next step over the edges of the faces [9]. Using this procedure a numerical code has been developed by P. Merkel.

The procedure described in this paper offers a systematic method to compute the magnetic field of modular coils to any required precision. By making use of the local coordinate system, the integration in the cross sectional plane can be carried through analytically leading to elementary

functions. The remaining integration along the coil axis requires numerical methods.

The magnetic field inside the coil is needed to compute the inductance of the coil and the magnetic energy. Furthermore, stress analysis of the coils requires the field inside the coil as input data. The maximum magnetic field occurs on the boundary of the winding pack. Since this number is limited by the critical field of the superconducting cables the computation of the maximum field is of great importance. Furthermore, a precise computation of the field is needed in the boundary region of magnetic surfaces where islands and stochasticity strongly depend on the details of the magnetic field.

2 Geometry of modular coils

In order to compute the magnetic field of a modular coil we start from the following assumptions: The perpendicular dimensions of the coil are small compared with the average radius, the local radius of curvature is large compared with the coil cross section. The coil can be approximated by a curved bar with a central axis described by $\boldsymbol{x} = \boldsymbol{X}_0(s)$ where s is the length along the central axis and $\boldsymbol{t}(s)$ the tangent vector, $\boldsymbol{n}(s)$ and $\boldsymbol{b}(s)$ are two orthogonal unit vectors in the cross-sectional plane perpendicular to the coil axis (see fig.(2). The normal vector $\boldsymbol{n}(s)$, in general, does not coincide with the natural coordinate system defined by the normal vector $\boldsymbol{n}_0(s)$ of the central filament. For technical reasons the spatial orientation of the coil cross section can deviate from the intrinsic normal vector. In fig.(1) the red satellite curve serves as the guide line defining the normal vector $\boldsymbol{n}(s)$. This defines a new coordinate system which is centered on the coil axis. The coil axis (or central filament)in the analysis is defined by the geometric center of the cross-sectional plane. Any point in the vicinity of the coil axis can be represented as

$$\boldsymbol{X} = \boldsymbol{X}_0(s) + y\boldsymbol{n}(s) + x\boldsymbol{b}(s) \quad , \quad \boldsymbol{t}(s) = \frac{d\boldsymbol{X}_0(s)}{ds} \tag{3}$$

This provides us with a coordinate transformation $X, Y, Z \Rightarrow s, y, x$ which is unique in a finite neighbourhood of the coil axis. In general, the unit vectors $\boldsymbol{n}(s), \boldsymbol{b}(s)$ do not coincide with the natural coordinate system in the cross-sectional plane. Let be $\boldsymbol{n}_0(s), \boldsymbol{b}_0(s)$ the normal and binormal vector of the central filament, where $\boldsymbol{n}_0$ points towards the center of curvature and $\boldsymbol{b}_0(s)$ is the bi-normal vector. The pair $\boldsymbol{n}(s), \boldsymbol{b}(s)$ is a linear combination of $\boldsymbol{n}_0(s), \boldsymbol{b}_0(s)$

$$\boldsymbol{n}(s) = \cos\alpha(s)\,\boldsymbol{n}_0(s) + \sin\alpha(s)\,\boldsymbol{b}_0(s), \quad \boldsymbol{b}(s) = \cos\alpha(s)\,\boldsymbol{b}_0(s) - \sin\alpha(s)\,\boldsymbol{n}_0(s) \tag{4}$$

The angle α describes the rotation of the coil with respect to its natural coordinate system. The inverse transformation is

$$\boldsymbol{n}_0(s) = \cos\alpha\,\boldsymbol{n}(s) - \sin\alpha\,\boldsymbol{b}(s), \quad \boldsymbol{b}_0(s) = \sin\alpha\,\boldsymbol{n}(s) + \cos\alpha\,\boldsymbol{b}(s) \tag{5}$$

In a coil with rectangular cross section the vectors $\boldsymbol{n}(s), \boldsymbol{b}(s)$ are parallel to the boundary of the coil. The derivatives of $\boldsymbol{n}_0(s), \boldsymbol{b}_0(s)$ are described by Frenets equations

$$\frac{d\boldsymbol{t}}{ds} = \kappa\,\boldsymbol{n}_0(s), \quad \frac{d\boldsymbol{b}_0}{ds} = \tau\,\boldsymbol{n}_0(s), \quad \frac{d\boldsymbol{n}_0}{ds} = -\kappa\,\boldsymbol{t}(s) - \tau\boldsymbol{b}_0 \tag{6}$$

which allow us to compute the scalar products

$$-\frac{d\boldsymbol{t}}{ds}\cdot\boldsymbol{b} = \frac{d\boldsymbol{b}}{ds}\cdot\boldsymbol{t} = \kappa\sin\alpha =: \gamma_3, \quad \frac{d\boldsymbol{t}}{ds}\cdot\boldsymbol{n} = -\frac{d\boldsymbol{n}}{ds}\cdot\boldsymbol{t} = \kappa\cos\alpha =: -\gamma_2 \tag{7}$$

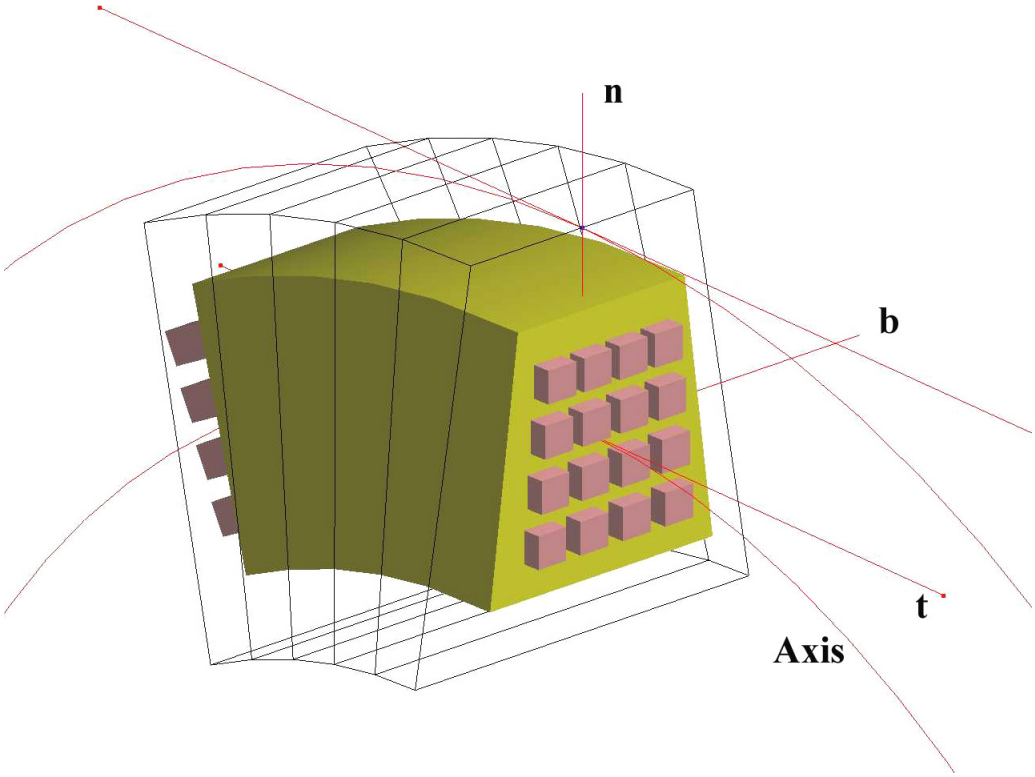

Figure 2: Section of modular coil. The winding pack is shown in yellow, the superconducting cable in red, the coil casing in wire frame. The local coordinate system is attached to the axis of the coil. Central filament and base vectors $\boldsymbol{t}, \boldsymbol{n}, \boldsymbol{b}$. In the following analysis we neglect the discreteness of the winding pack and describe the current density in the winding pack by a continuous function.

and

$$\frac{d\boldsymbol{n}}{ds} \cdot \boldsymbol{b} = -\frac{d\boldsymbol{b}}{ds} \cdot \boldsymbol{n} = \frac{d\alpha}{ds} - \tau := \gamma_1 \tag{8}$$

$\kappa(s)$ and $\tau(s)$ are the curvature and the torsion of the coil axis, $\alpha(s)$ is the angle between the normal vector $\boldsymbol{n}(s)$ of the coil and the normal vector $\boldsymbol{n}_0(s)$ of the coil axis. The derivatives of the base vectors are given by

$$\begin{pmatrix} \boldsymbol{n}'(s) \\ \boldsymbol{b}'(s) \\ \boldsymbol{t}'(s) \end{pmatrix} = \begin{pmatrix} 0 & \gamma_1 & \gamma_2 \\ -\gamma_1 & 0 & \gamma_3 \\ -\gamma_2 & -\gamma_3 & 0 \end{pmatrix} \begin{pmatrix} \boldsymbol{n}(s) \\ \boldsymbol{b}(s) \\ \boldsymbol{t}(s) \end{pmatrix} \tag{9}$$

The matrix $\gamma_{ik}(s)$ is antisymmetric, it describes the geometry of the coils, its curvature and torsion. In a plane circular coil the coefficients are $\gamma_1 = \gamma_3 = 0, \quad \gamma_2 = -\kappa$. By introducing the following notation $\boldsymbol{e}_0 = \boldsymbol{n}, \boldsymbol{e}_1 = \boldsymbol{b}, \boldsymbol{e}_2 = \boldsymbol{t}$ we may write eq. (9) in the form

$$\boldsymbol{e}_i' = \sum_k \gamma_{ik} \boldsymbol{e}_k \tag{10}$$

3 The local coordinate system

In the following chapter we investigate the local coordinate system in more detail and compute the metric elements of the transformation from global to local coordinates. The derivatives of

the transformation $\boldsymbol{X} \Leftrightarrow s, y, x$ are

$$\delta_{ik} = \left(\boldsymbol{t}_i + y\boldsymbol{n}_i' + x\boldsymbol{b}_i'\right) \frac{\partial s}{\partial X_k} + \boldsymbol{n}_i \frac{\partial y}{\partial X_k} + \boldsymbol{b}_i \frac{\partial x}{\partial X_k} \tag{11}$$

and

$$\nabla s = \frac{\boldsymbol{t}(s)}{\left(1 + y\boldsymbol{n}' \cdot \boldsymbol{t} + x\boldsymbol{b}' \cdot \boldsymbol{t}\right)}, \quad \boldsymbol{n} = x\,\boldsymbol{b}' \cdot \boldsymbol{n}\nabla s + \nabla y, \quad \boldsymbol{b} = y\,\boldsymbol{n}' \cdot \boldsymbol{b}\nabla s + \nabla x \tag{12}$$

while the derivatives of X, Y, Z with respect to s, y, x provide us with the relation

$$\frac{\partial \boldsymbol{X}}{\partial s} = \boldsymbol{t}(s) + y\boldsymbol{n}'(s) + x\boldsymbol{b}'(s), \quad \frac{\partial \boldsymbol{X}}{\partial y} = \boldsymbol{n}(s), \quad \frac{\partial \boldsymbol{X}}{\partial x} = \boldsymbol{b}(s) \tag{13}$$

Inserting this result into eq.(12) leads to

$$\nabla s = \frac{\boldsymbol{t}(s)}{(1 + y\gamma_2 + x\gamma_3)}; \quad \nabla y = \boldsymbol{n}(s) + x\gamma_1\nabla s \quad \nabla x = \boldsymbol{b}(s) - y\gamma_1\nabla s \tag{14}$$

Furthermore, we compute the scalar products

$$\begin{aligned}
\nabla s \cdot \boldsymbol{t} &= \frac{1}{1 + y\gamma_2 + x\gamma_3}, \quad \nabla s \cdot \boldsymbol{n} = 0, \quad \nabla s \cdot \boldsymbol{b} = 0 \\
\nabla y \cdot \boldsymbol{t} &= \frac{x\gamma_1}{1 + y\gamma_2 + x\gamma_3}, \quad \nabla y \cdot \boldsymbol{n} = 1, \quad \nabla y \cdot \boldsymbol{b} = 0 \\
\nabla x \cdot \boldsymbol{t} &= -\frac{y\gamma_1}{1 + y\gamma_2 + x\gamma_3}, \quad \nabla x \cdot \boldsymbol{n} = 0, \quad \nabla x \cdot \boldsymbol{b} = 1
\end{aligned} \tag{15}$$

In addition, we will need the following differential operators

$$\boldsymbol{t} \cdot \nabla = (\boldsymbol{t} \cdot \nabla s)\left[\frac{\partial}{\partial s} + \gamma_1\left(x\frac{\partial}{\partial y} - y\frac{\partial}{\partial x}\right)\right]; \quad \boldsymbol{n} \cdot \nabla = \frac{\partial}{\partial y}; \quad \boldsymbol{b} \cdot \nabla = \frac{\partial}{\partial x} \tag{16}$$

The divergence of the base vectors is

$$\nabla \cdot \boldsymbol{t} = 0, \quad \nabla \cdot \boldsymbol{b} = \frac{\gamma_3}{1 + y\gamma_2 + x\gamma_3}, \quad \nabla \cdot \boldsymbol{n} = \frac{\gamma_2}{1 + y\gamma_2 + x\gamma_3} \tag{17}$$

The derivative $\boldsymbol{X}_s$ is

$$\frac{\partial \boldsymbol{X}}{\partial s} = (1 + y\gamma_2 + x\gamma_3)\,\boldsymbol{t}(s) + y\gamma_1\boldsymbol{b}(s) - x\gamma_1\boldsymbol{n}(s) \tag{18}$$

and the metric elements of the transformation are

$$h_s^2 := \left|\frac{\partial \boldsymbol{X}}{\partial s}\right|^2 = (1 + y\gamma_2 + x\gamma_3)^2 + \gamma_1^2\left(x^2 + y^2\right), \quad \left|\frac{\partial \boldsymbol{X}}{\partial y}\right| = 1, \quad \left|\frac{\partial \boldsymbol{X}}{\partial x}\right| = 1 \tag{19}$$

The length element is

$$dS^2 = \begin{pmatrix} ds \\ dx \\ dy \end{pmatrix} \cdot \begin{pmatrix} h_s^2 & y\gamma_1 & -x\gamma_1 \\ y\gamma_1 & 1 & 0 \\ -x\gamma_1 & 0 & 1 \end{pmatrix} \begin{pmatrix} ds \\ dx \\ dy \end{pmatrix} \tag{20}$$

and the metric elements of the transformation are

$$g_{ss} = h_s^2, \quad g_{xx} = g_{yy} = 1, \quad g_{xy} = 0, \quad g_{sx} = y\gamma_1, \quad g_{sy} = -x\gamma_1 \tag{21}$$

and the volume element is

$$dV = \sqrt{g}\,dydxds = \sqrt{h_s^2 - \gamma_1^2(x^2 + y^2)}\,dydxds = (1 + \gamma_2 y + \gamma_3 x)\,dydxds \tag{22}$$

Note, that the volume element is linear in x, y, the coordinates in the cross sectional plane. This is a useful property in view of the 2-D integration in the cross-sectional plane.

4 Magnetic field

The magnetic field of a modular coil depends on the geometry of the coil and the current density. In a coil with rectangular cross section (height $2h$, width $2b$) the current density is constant and can be written as $\boldsymbol{j} = |\boldsymbol{j}|\boldsymbol{t}$. A trapezoidal shape of the cross section helps to reduce the maximum field on the coil. In this case the current density is not constant but varies with height of the coil. Let be $b(y) = b_0(1 - ky)$, $-h \le y \le h$, $k = \text{const.}$ the width of a trapezoidal coil and $j(y)$ the current density. One option to the reduce the current density is $j(y)b(y) = \text{const}$. We may use the approximation

$$j(y) = \frac{1}{1-ky} j(0) \approx j(0)(1+ky), \quad k \ll 1 \tag{23}$$

The total current is

$$I = \int j(y)\, dydx = \int_h^h j(y)dy \int_{-b(y)}^{b(y)} dx = 4hb_0 j(0) \tag{24}$$

In the following we analyse the case of constant current density and a rectangular cross section. The vector potential of the magnetic field is

$$\boldsymbol{A}(\boldsymbol{X}) = \frac{\mu_0}{4\pi} \int \frac{\boldsymbol{j}(\boldsymbol{x})}{|\boldsymbol{X}-\boldsymbol{x}|}\, d^3\boldsymbol{x} = \frac{\mu_0|\boldsymbol{j}|}{4\pi} \int \frac{\boldsymbol{t}}{|\boldsymbol{X} - \boldsymbol{X}_0(s) - y\boldsymbol{n} - x\boldsymbol{b}|} \frac{dydxds}{|\nabla s|} \tag{25}$$

and the magnetic field is

$$\boldsymbol{B}(\boldsymbol{X}) = \frac{\mu_0}{4\pi} \int \frac{\boldsymbol{j} \times (\boldsymbol{X}-\boldsymbol{x})}{|\boldsymbol{X}-\boldsymbol{x}|^3}\, d^3\boldsymbol{x} = \frac{\mu_0|\boldsymbol{j}|}{4\pi} \int \frac{\boldsymbol{t} \times (\boldsymbol{X} - \boldsymbol{X}_0(s) - y\boldsymbol{n} - x\boldsymbol{b})}{|\boldsymbol{X} - \boldsymbol{X}_0(s) - y\boldsymbol{n} - x\boldsymbol{b}|^3} \frac{dydxds}{|\nabla s|} \tag{26}$$

The denominator in the integral has the structure

$$N(\boldsymbol{X}, s, y, x) := |\boldsymbol{X} - \boldsymbol{X}_0(s) - y\boldsymbol{n} - x\boldsymbol{b}| = \sqrt{s_0^2 + (y-y_0)^2 + (x-x_0)^2} \tag{27}$$

In local coordinates the point $\boldsymbol{X} - \boldsymbol{X}_0(s)$ has the components

$$s_0(s) = (\boldsymbol{X} - \boldsymbol{X}_0(s)) \cdot \boldsymbol{t}, \quad y_0(s) = (\boldsymbol{X} - \boldsymbol{X}_0(s)) \cdot \boldsymbol{n}, \quad x_0(s) = (\boldsymbol{X} - \boldsymbol{X}_0(s)) \cdot \boldsymbol{b} \tag{28}$$

and has the representation

$$\boldsymbol{X} - \boldsymbol{X}_0(s) = s_0\boldsymbol{t} + y_0\boldsymbol{n} + x_0\boldsymbol{b} \quad , \quad R_0 = |\boldsymbol{X} - \boldsymbol{X}_0(s)| = \sqrt{s_0^2 + y_0^2 + x_0^2} \tag{29}$$

and

$$\boldsymbol{t} \times (\boldsymbol{X} - \boldsymbol{X}_0(s) - y\boldsymbol{n} - x\boldsymbol{b}) = (y-y_0)\boldsymbol{b} - (x-x_0)\boldsymbol{n} \tag{30}$$

4.0.1 Vector potential

In computing the vector potential we need the following integrals over the coil cross section

$$F_1 = \int \frac{1}{N(\boldsymbol{X}, s, y, x)}\, dydx, \quad F_2 = \int \frac{y-y_0}{N(\boldsymbol{X}, s, y, x)}\, dydx, \quad F_3 = \int \frac{x-x_0}{N(\boldsymbol{X}, s, y, x)}\, dydx \tag{31}$$

and the function

$$g(\boldsymbol{X}, s) = \int \frac{1}{N(\boldsymbol{X}, s, y, x)} \frac{dydx}{|\nabla s|} = F_1 + \gamma_2(y_0F_1 + F_2) + \gamma_3(x_0F_1 + F_3) \tag{32}$$

The region of integration is $-h \le y \le h, -b \le x \le b$. The vector potential reads

$$\boldsymbol{A}(\boldsymbol{X}) = \frac{|\boldsymbol{j}|\mu_0}{4\pi} \oint \boldsymbol{t}(s) g(\boldsymbol{X}, s)\, ds \tag{33}$$

In a planar coil $\gamma_3 = 0$ the vector potential is

$$\boldsymbol{A}(\boldsymbol{X}) = \frac{|\boldsymbol{j}|\mu_0}{4\pi} \oint \boldsymbol{t}(s) \left(F_1 + \gamma_2(y_0 F_1 + F_2)\right) ds \tag{34}$$

In a straight rectangular bar ($\gamma_2 = 0, \gamma_3 = 0$) this reduces to

$$\boldsymbol{A}(\boldsymbol{X}) = \frac{|\boldsymbol{j}|\mu_0}{4\pi} \oint \boldsymbol{t}(s) F_1(\boldsymbol{X}, s)\, ds \tag{35}$$

At large distance form the coil ($|y| \ll y_0, |x| \ll x_0$) we may approximate $N(\boldsymbol{X}, s, y, x)$ by $N(\boldsymbol{X}, s, 0, 0)$ and and compute the magnetic field by Biot-Savart's law. In order to find an estimate of the error we expand the function $1/N$

$$\frac{1}{N} = \frac{1}{\sqrt{R_0^2 + q}} = \frac{1}{R_0}\left[1 - \frac{1}{2}\frac{q}{R_0^2} + \frac{3}{8}\frac{q^2}{R_0^4} - \frac{15}{48}\frac{q^3}{R_0^6} + ...\right] \quad ; \quad q = y(y - 2y_0) + x(x - 2x_0) \tag{36}$$

With the help of this expansion the series expansion of the functions $F_1, ...F_3$ can be computed; the details are described in appendix 1. In order to estimate the error of the lowest order approximation we consider the expansion of F_1.

$$F_1 = \frac{M_{0,0}}{R_0}\left[1 - \frac{1}{6}\frac{h^2 + b^2}{R_0^2} + ...\right] \quad ; \quad M_{0,0} = 4hb \tag{37}$$

As an example we consider a quadratic cross section $h = b$ and a distance $R_0 = 6h$. In this case the first order term is of the order 10^{-2}. This example shows that the Biot-Savart approximation is good enough to compute $|B|$ in the far neighbourhood of the coil, however, the structure of magnetic surfaces strongly depends on the precise computation of the magnetic field. In particular, in the boundary region of magnetic surfaces, where islands and stochastic regions occur, higher order corrections in F_k must be taken into account. The error in computing the magnetic field should be less than 10^{-4}.

4.0.2 Magnetic field

The magnetic field of a rectangular coil with constant current density is

$$\boldsymbol{B}(\boldsymbol{X}) = \frac{|\boldsymbol{j}|\mu_0}{4\pi} \int \frac{(y - y_0)\boldsymbol{b} - (x - x_0)\boldsymbol{n}}{N^3(\boldsymbol{X}, s, y, x)} \frac{dydxds}{|\nabla s|} \tag{38}$$

If the distance $|\boldsymbol{X} - \boldsymbol{X}_0|$ is large enough the current density may be approximated by a delta-function $|\boldsymbol{j}| = I_0\delta(x)\delta(y)$ and the magnetic field is given by Biot-Savart's law.

$$\boldsymbol{B}(\boldsymbol{X}) = \frac{\mu_0 I_0}{4\pi} \oint \frac{x_0\boldsymbol{n} - y_0\boldsymbol{b}}{R_0^3(\boldsymbol{X}, s)}\, ds \tag{39}$$

Introducing the following integrals

$$F_4 = \int \frac{(y - y_0)dydx}{N^3(\boldsymbol{X}, s, y, x)}, \quad F_5 = \int \frac{(x - x_0)dydx}{N^3(\boldsymbol{X}, s, y, x)}, \quad F_6 = \int \frac{(y - y_0)(x - x_0)}{N^3(\boldsymbol{X}, s, y, x)}\, dydx \tag{40}$$

and

$$F_7 = \int \frac{(y-y_0)^2 dydx}{N^3(\boldsymbol{X},s,y,x)}\,, \quad F_8 = \int \frac{(x-x_0)^2 dydx}{N^3(\boldsymbol{X},s,y,x)} \tag{41}$$

allows us to write the magnetic field as line integral on the coil axis

$$\begin{aligned} \boldsymbol{B}(\boldsymbol{X}) &= \frac{\mu_0|\boldsymbol{j}|}{4\pi}\oint \left[(1+\gamma_2 y_0+\gamma_3 x_0)F_4+\gamma_2 F_7+\gamma_3 F_6\right]\boldsymbol{b}\,ds \\ &- \frac{\mu_0|\boldsymbol{j}|}{4\pi}\oint \left[1+\gamma_2 y_0+\gamma_3 x_0)F_5+\gamma_2 F_6+\gamma_3 F_8\right]\boldsymbol{n}\,ds \end{aligned} \tag{42}$$

or

$$\begin{aligned} \boldsymbol{B}(\boldsymbol{X}) &= \frac{\mu_0|\boldsymbol{j}|}{4\pi}\oint \left[F_4+\gamma_2(y_0F_4+F_7)+\gamma_3(x_0F_4+F_6)\right]\boldsymbol{b}\,ds \\ &- \frac{\mu_0|\boldsymbol{j}|}{4\pi}\oint \left[F_5+\gamma_2(y_0F_5+F_6)+\gamma_3(x_0F_5+F_8)\right]\boldsymbol{n}\,ds \end{aligned} \tag{43}$$

In a straight bar the magnetic field is

$$\boldsymbol{B}(\boldsymbol{X}) = \frac{\mu_0}{4\pi}\oint \left[F_4\boldsymbol{b}-F_5\boldsymbol{n}\right]ds \tag{44}$$

This approximation is used in the EFFI-code [2], where the coil is approximated by a number of straight segments. In appendix 8.2 an analytic formulation will be derived. A planar circular coil ($\gamma_2 = 1/R, \gamma_3 = 0$) is described by

$$\begin{aligned} \boldsymbol{B}(\boldsymbol{X}) &= \frac{\mu_0|\boldsymbol{j}|}{4\pi}\oint \left[F_4+\gamma_2(y_0F_4+F_7)\right]\boldsymbol{b}\,ds \\ &- \frac{\mu_0|\boldsymbol{j}|}{4\pi}\oint \left[F_5+\gamma_2(y_0F_5+F_6)\right]\boldsymbol{n}\,ds \end{aligned} \tag{45}$$

The functions F_4, F_5 are zero at $x_0 = 0, y_0$ for any s_0, which implies that the magnetic field of a straight bar is zero at the center. The comparison of eq.44 and eq.45 demonstrates that an approximation by straight sections - as done in the EFFI-code - leads to erroneous results. The curvature γ_2 of the coil introduces some additional terms.

The series expansion

$$\frac{1}{N^3} = \frac{1}{R_0^3}\left[1-\frac{3}{2}\frac{q}{R_0^2}+\frac{15}{8}\frac{q^2}{R_0^4}-\frac{245}{48}\frac{q^3}{R_0^6}+...\right] \tag{46}$$

will be used to compute an approximation of the field (see appendix 1). There is a relation between the functions F_k

$$\begin{aligned} F_6 &= \int y(x-x_0)\,\frac{dxdy}{N^3} - y_0F_5 \\ F_7 &= \int y(y-y_0)\,\frac{dxdy}{N^3} - y_0F_4 \\ F_8 &= \int x(x-x_0)\,\frac{dxdy}{N^3} - x_0F_5 \end{aligned} \tag{47}$$

As shown in the appendix the functions $F_1, ..., F_8$ can be written in terms of elementary functions, thus reducing the computation of the magnetic field to an one-dimensional integration over s.

A numerical computation of the magnetic field is faced with the singularity in the functions $F_1 ... F_8$. This singularity of $1/N$ exists inside the coil at $s_0 = 0$ and a point x_0, y_0 inside the coil cross section. Given the field point $\boldsymbol{X}$ the components are functions of $s: x_0 = x_0(s), y_0 = y_0(s), s_0 = s_0(s)$. The condition $s_0(S) = 0$ defines the critical cross section $s = S$, where the singularity occurs, if the point $\boldsymbol{X}$ is inside the coil winding pack. Let us consider F_4 and decompose the region of integration $\Delta: -b \le x \le b, -h \le y \le h$ into $\Delta = \Delta[a] + (\Delta - \Delta[a]$. $\Delta[a] \subset \Delta$ is a square enclosed in Δ and centered to x_0, y_0. a is the side length of the square.

$$F_4 = \int_\Delta \frac{(y-y_0)dydx}{N^3(\boldsymbol{X},s,y,x)} = \int_{\Delta[a]} \frac{(y-y_0)dydx}{N^3(\boldsymbol{X},s,y,x)} + \int_{\Delta-\Delta[a]} \frac{(y-y_0)dydx}{N^3(\boldsymbol{X},s,y,x)} \tag{48}$$

The second integral on the right hand side does not enclose the singularity and it is finite for any s_0. The first integral on the right hand side, however, is zero for any s_0 since the integrand in y is antisymmetric in $\Delta[a]$. We set $F_4(s_0 = 0) = \lim_{s_0 \to 0} F_4(s_0)$. The same arguements apply to F_2, F_3, F_5, F_6. In F_1, F_7, F_8 the integrand of the first integral is symmetric and the integral is finite. Let be $\Delta[a] \subset \Delta$ a circle with radius a, and, after introducing polar coordinates we get

$$\begin{aligned} F_1 = \int_\Delta \frac{dydx}{N(\boldsymbol{X},s,y,x)} &= \int_{\Delta[a]} \frac{r dr\, d\varphi}{\sqrt{s_0^2 + r^2}} + \int_{\Delta-\Delta[a]} \frac{dydx}{N(\boldsymbol{X},s,y,x)} \\ &= 2\pi \left(\sqrt{s_0^2 + a^2} - \sqrt{s_0^2} \right) + \int_{\Delta-\Delta[a]} \frac{dydx}{N(\boldsymbol{X},s,y,x)} \end{aligned} \tag{49}$$

The integral is finite for any s_0. In case of F_7 we find

$$F_7 = \int_\Delta \frac{(y-y_0)^2 dydx}{N^3(\boldsymbol{X},s,y,x)} = \int_{\Delta[a]} \frac{r^3 dr\, \sin^2\varphi\, d\varphi}{\left[\sqrt{s_0^2 + r^2}\right]^3} + \int_{\Delta-\Delta[a]} \frac{(y-y_0)^2 dydx}{N^3(\boldsymbol{X},s,y,x)} \tag{50}$$

The integration over the circle yields a finite result and the limit $s_0 \to 0$ is

$$F_7 = \int_\Delta \frac{(y-y_0)^2 dydx}{N^3(\boldsymbol{X},s,y,x)} = a\pi + \int_{\Delta-\Delta[a]} \frac{(y-y_0)^2 dydx}{N^3(\boldsymbol{X},s,y,x)} \tag{51}$$

A similar result holds for F_8

$$F_8 = \int_\Delta \frac{(x-x_0)^2 dydx}{N^3(\boldsymbol{X},s,y,x)} = a\pi + \int_{\Delta-\Delta[a]} \frac{(x-x_0)^2 dydx}{N^3(\boldsymbol{X},s,y,x)}. \tag{52}$$

In the case of an inhomogeneous current density $j = j(0)(1+ky)$ the functions $F_1, ..., F_8$ will be modified. Instead of F_1 we get

$$F_1 = \int_{-h}^{h} \int_{-b(y)}^{b(y)} \frac{j(y)}{N(\boldsymbol{X},s,y,x)}\, dydx = \int_{-h}^{h} \int_{-b(y)}^{b(y)} \frac{1+ky}{N(\boldsymbol{X},s,y,x)}\, dydx \tag{53}$$

The integration in x extends from $-b(y)$ to $b(y)$. Everywhere in F_k we must replace $dydx$ by $(1+ky)dydx$. Integration over x is still possible, however the integration over y cannot be made with the help of elementary functions.

The magnetic energy of a coil with a rectangular winding pack is

$$E_m = \int \frac{B^2}{2}\, d^3\boldsymbol{x} = \frac{1}{2} \int \boldsymbol{j} \cdot \boldsymbol{A}\, d^3\boldsymbol{x} = \frac{|\boldsymbol{j}|^2}{8\pi} \oint \oint \boldsymbol{t}(s) \cdot \boldsymbol{t}(s') \int g(s') \frac{dxdy}{|\nabla s|}\, dsds' \tag{54}$$

This result may be used to compute the inductivity of the coil.

5 Approximative field computation

The numerical computation of the magnetic field is faced with a strong peaking or a logarithmic singularity of the functions $F_4, ..F_8$ if the field point $\boldsymbol{X}$ is close to or inside the coil. The EFFI-code [2] decomposes the coil in a set of straight sections and and utilizes analytic solutions of straight sections as described in appendix 9.2. In the following we describe a modified procedure which accounts for the curvature of the coils. For this purpose we approximate the axis of the coil by a polygon defined a finite number of points $\boldsymbol{X}_0(s_i)$, $i = 0, ..., N$. Let the segments $\Delta s_i = s_{i+1} - s_i$ be small enough so that the variation of the functions $\gamma_2(s), \gamma_3(s), x_0(s), y_0(s)$ in the segments is negligeable and can be replaced by a mean value. Furthermore, the normal and bi-normal vectors are replaced by their mean values in Δs_i. However, the functions $F_1, .., F_8$ may strongly vary in the segments, in particular in the neighbourhood of the field point. Under these assumptions the magnetic field can be written as a sum over all segments

$$\begin{aligned}
\boldsymbol{B}(\boldsymbol{X}) &= \frac{\mu_0|\boldsymbol{j}|}{4\pi}\sum_k \left[\oint F_4\,ds + \gamma_2\oint (y_0F_4 + F_7)\,ds + \gamma_3\oint (x_0F_4 + F_6)\,ds\right]\overline{\boldsymbol{b}} \\
&- \frac{\mu_0|\boldsymbol{j}|}{4\pi}\sum_k \left[\oint F_5\,ds + \gamma_2\oint (y_0F_5 + F_6)\,ds + \gamma_3\oint (x_0F_5 + F_8)\,ds\right]\overline{\boldsymbol{n}} \qquad (55)
\end{aligned}$$

The integration over s runs over the functions $F_4, .., F_8$ only. The integration of F_4 and F_5 is described in appendix 8.2 and leads to analytic functions. In the following we describe a procedure which reduces the numerical computation to an one-dimensional integration. In the segment Δ_i we may identify the length s with s_0 and the integration over s yields

$$\int_{\Delta_i} \frac{ds}{N^3(\boldsymbol{X}, s, y, x)} = \frac{s}{[(y-y_0)^2 + (x-x_0)^2]\sqrt{s^2 + (y-y_0)^2 + (x-x_0)^2}} + C \qquad (56)$$

and

$$\int_{\Delta_i} \frac{ds}{N(\boldsymbol{X}, s, y, x)} = \ln\left(s + \sqrt{s^2 + (y-y_0)^2 + (x-x_0)^2}\right) + C \qquad (57)$$

With regard to the x, y-integration we introduce polar coordinates centered to $x_0, y_0 : x - x_0 = r\cos\varphi, y - y_0 = r\sin\varphi$. The transformation yields

$$\begin{aligned}
\int F_1\,ds &= \int \ln\left(s + \sqrt{s^2 + r^2}\right)\, r dr d\varphi + C \\
\int F_2\,ds &= \int \ln\left(s + \sqrt{s^2 + r^2}\right)\sin\varphi\, r^2 dr d\varphi + C \\
\int F_3\,ds &= \int \ln\left(s + \sqrt{s^2 + r^2}\right)\cos\varphi\, r^2 dr d\varphi + C \qquad (58)
\end{aligned}$$

The integration over r runs from $r = 0$ to $r = r(\varphi)$ and can be carried through analytically

$$\begin{aligned}
M_1(s, r) : &= \int \ln\left(s + \sqrt{s^2 + r^2}\right)\, r dr \\
&= \frac{r^2}{2}\ln\left(s + \sqrt{s^2 + r^2}\right) - \frac{r^2}{4} + \frac{s}{2}\left(\sqrt{s^2 + r^2} - \sqrt{s^2}\right) \qquad (59)
\end{aligned}$$

and

$$\begin{aligned}
M_2(s, r) := \int \ln\left(s + \sqrt{s^2 + r^2}\right)\, r^2 dr &= \frac{r^3}{3}\ln\left(s + \sqrt{s^2 + r^2}\right) - \frac{r^3}{9} + \frac{sr}{3}\sqrt{s^2 + r^2} \\
&- \frac{sr}{6} - \frac{s^3}{6}\left(\ln\left(r + \sqrt{s^2 + r^2}\right) - \ln\sqrt{s^2}\right) \qquad (60)
\end{aligned}$$

$r = r(\varphi)$ is the distance between the point x_0, y_0 and the boundary of the winding pack. With the help of these results we get

$$\begin{aligned}
\int_{s1}^{s2} F_1\, ds &= \int \{M_1(s_2, r(\varphi)) - M_1(s_1, r(\varphi))\}\, d\varphi \\
\int_{s_1}^{s_2} F_2\, ds &= \int \{M_2(s_2, r(\varphi) - M_2(s_1, r(\varphi)\} \sin\varphi\, d\varphi \\
\int_{s_1}^{s_2} F_3\, ds &= \int \{M_2(s_2, r(\varphi)) - M_2(s_1, r(\varphi))\} \cos\varphi\, d\varphi
\end{aligned} \tag{61}$$

s_2, s_1 are the limits of the segment. Integrating the functions $F_4, ..., F_8$ yields

$$\int F_4\, ds = s \int \frac{\sin\varphi\, dr d\varphi}{\sqrt{s^2 + r^2}}, \quad \int F_5\, ds = s \int \frac{\cos\varphi\, dr d\varphi}{\sqrt{s^2 + r^2}}, \quad \int F_6\, ds = s \int \frac{\cos\varphi \sin\varphi\, r dr d\varphi}{\sqrt{s^2 + r^2}} \tag{62}$$

and

$$\int F_7\, ds = s \int \frac{\sin\varphi \sin\varphi\, r dr d\varphi}{\sqrt{s^2 + r^2}} \quad , \quad \int F_8\, ds = s \int \frac{\cos\varphi \cos\varphi\, r dr d\varphi}{\sqrt{s^2 + r^2}} \tag{63}$$

The integration over r between $r = 0$ and $r = r(\varphi)$ leads to

$$M_3(s, r) = s \int \frac{dr}{\sqrt{s^2 + r^2}} = s \left(\ln(r + \sqrt{s^2 + r^2}) - \ln(\sqrt{s^2}) \right) \tag{64}$$

and

$$M_4(s, r) = s \int \frac{r dr}{\sqrt{s^2 + r^2}} = s \left(\sqrt{s^2 + r^2} - \sqrt{s^2} \right) \tag{65}$$

The final result is

$$\begin{aligned}
\int_{s_1}^{s_2} F_4\, ds &= \int \{M_3(s_2, r(\varphi)) - M_3(s_1, r(\varphi))\} \sin\varphi\, d\varphi \\
\int_{s_1}^{s_2} F_5\, ds &= \int \{M_3(s_2, r(\varphi)) - M_3(s_1, r(\varphi))\} \cos\varphi\, d\varphi \\
\int_{s_1}^{s_2} F_6\, ds &= \int \{M_4(s_2, r(\varphi)) - M_4(s_1, r(\varphi))\} \sin\varphi \cos\varphi\, d\varphi \\
\int_{s_1}^{s_2} F_7\, ds &= \int \{M_4(s_2, r(\varphi)) - M_4(s_1, r(\varphi))\} \sin\varphi \sin\varphi\, d\varphi \\
\int_{s_1}^{s_2} F_8\, ds &= \int \{M_4(s_2, r(\varphi)) - M_4(s_1, r(\varphi))\} \cos\varphi \cos\varphi\, d\varphi
\end{aligned} \tag{66}$$

The integration over φ runs from zero to 2π if the point x_0, y_0 lies inside the winding pack ($x_0, y_0 \in \Delta$). If the point is outside Δ the limits depend on x_0, y_0. If the point x_0, y_0 lies on the boundary the integration runs from $-\pi$ to π. The distance $r(\varphi)$ is is zero at some angle φ_0. The preceding formulation holds for any shape of the cross section, it is not restricted to a rectangular shape. In a straight rectangular bar we only need the integration over F_4, F_5 which are given in appendix 9.2 eqs.103,104. This is the approximation used in the EFFI-code, however, the curvature of the coil introduces some additional terms.

The integration over F_4 ad F_5 can be done analytically if the cross section is rectangular. The result is

$$
\begin{aligned}
\int_{s_1}^{s_2} F_4\,ds &= -\int_{s_1}^{s_2} F(b-x_0,h-y_0,s)\,ds - \int_{s_1}^{s_2} F(-b-x_0,-h-y_0,s)\,ds \\
&+ \int_{s_1}^{s_2} F(-b-x_0,h-y_0,s)\,ds + \int_{s_1}^{s_2} F(b-x_0,-h-y_0,s)\,ds \\
&= -I(b-x_0,h-y_0,s_2) - I(-b-x_0,-h-y_0,s_2) \\
&+ I(-b-x_0,h-y_0,s_2) + I(b-x_0,-h-y_0,s_2) \\
&+ I(b-x_0,h-y_0,s_1) + I(-b-x_0,-h-y_0,s_1) \\
&- I(-b-x_0,h-y_0,s_1) - I(b-x_0,-h-y_0,s_1) \qquad (67)
\end{aligned}
$$

and

$$
\begin{aligned}
\int_{s_1}^{s_2} F_5\,ds &= -I(h-y_0,b-x_0,s_2) - I(-h-y_0,-b-x_0,s_2) \\
&+ I(-h-y_0,b-x_0,s_2) + I(h-y_0,-b-x_0,s_2) \\
&+ I(h-y_0,b-x_0,s_1) + I(-h-y_0,-b-x_0,s_1) \\
&- I(-h-y_0,b-x_0,s_1) - I(h-y_0,-b-x_0,s_1) \qquad (68)
\end{aligned}
$$

6 Numerical example

In the following we consider a circular coil with rectangular or trapezoidal cross section. The radius of the coil is 5 m and the current 10 MA. According to Biot-Savart's law the magnetic field at the coil center is $4\pi/10$ [T]. The magnetic field increases towards the coil and has its maximum on the boundary of the coil ($r/R = 0.8$). In order to achieve a precision of 10^{-4} all computations were made with double precision. The following table shows a comparison of the results by Biot-Savart and the numerical computation of a finite size coil. The cross section of the winding pack is defined by h, b_1, b_2, where $2h$ is the height of the winding pack and $2b_1 = 2b_2$ is the width of the rectangular winding pack. In case of a trapezoidal cross section the width is $b_1 \le b(y) \le b_2$.

The functions F_k are computed by two-dimensional Simpson integration, assuming the $s_0 \neq 0$ if the magnetic field inside the coil is computed. Given a point $\boldsymbol{X}$ the grid points s_k can be always be constructed so that $s_0(s_k) \neq 0$. Alternatively one can replace s_0^2 by $s_0^2 + \epsilon,\ 0 < \epsilon \ll 1$, which removes the singularity. In the external region of the coil the singularity of $1/N$ does not occur and no special procedure is needed. Increasing the number of grid point of the Simpson integration allows one to compute the magnetic field to any given precision. The following table displays the radial dependence of the magnetic field in a circular coil in the external region. First column: normalized radius, second column: magnetic field according to eq. (45), third column: Biot-Savart approximation, last column: difference in percent. The dimensions of the coil are: R =5 m, h=1 m, $b_1 = b_2$ =1 m, total current 10 MA.

Radius	B (Exact)	B (Biot-S.)	Difference [%]
0.00000000	1.24742304	1.25663706	0.73322883
0.05000000	1.24971858	1.25899879	0.73711024
0.10000000	1.25666775	1.26615106	0.74898753
0.15000000	1.26846240	1.27830013	0.76959455
0.20000000	1.28543705	1.29580712	0.80027903
0.25000000	1.30809290	1.31921686	0.84322474
0.30000000	1.33713548	1.34930414	0.90184738
0.35000000	1.37353084	1.38714554	0.98149079
0.40000000	1.41858735	1.43423011	1.09067282
0.45000000	1.47407362	1.49263275	1.24338211
0.50000000	1.54238548	1.56529302	1.46346685
0.55000000	1.62677381	1.65647999	1.79333116
0.60000000	1.73162677	1.77260424	2.31171008
0.65000000	1.86272721	1.92372136	3.17063325
0.70000000	2.02712411	2.12652718	4.67443257
0.75000000	2.22947911	2.41091746	7.52569713
0.80000000	2.41021697	2.83625028	15.02100533

The Biot-Savart approximation is slightly larger than the exact field. At $r/R = 0.5$ the difference is 1.46% and grows towards the winding pack to 15%. This result clearly shows that, if a precision of 10^{-4} is required, the Biot-Savart approximation is not sufficient. However, one must distinguish between the plasma boundary and the interior region. At the boundary islands and stochasticity occurs, and, since the island size strongly depends on the details of the magnetic field, this region requires the highest precision.

The maximum field on the coil is another issue, it should be as small as possible in order to prevent quenching of a superconducting coil. To reduce the current density in a coil at a fixed total current the cross section should be as large as possible. However, in a toroidal coil set a rectangular cross section is not the optimum choice, a trapezoidal cross section helps to reduce the maximum field and the current density, while the magnetic field in the plasma region remains nearly unchanged. The current density in a trapezoidal winding pack is inhomogeneous $j = j(y)$, in the following computations the density scales inversely with $b(y), j(y)b(y) = \text{const}$. In the previous example a trapezoidal shape ($h = 1$ m, $b_1 = 1$ m, $b_2 = 1.2$ m) reduces the maximum field from $B = 2.41$ to $B = 2.28$ T. If the cross section of the coil is smaller ($h = 0.5$ m, $b_1 = 0.5$ m, $b_2 = 0.5 \rightarrow 0.6$ m) the effect of field reduction is larger: $B_{max} = 4.293\text{T} \rightarrow 4.026$ T.

7 Summary and conclusions

A modular coil with rectangular or trapezoidal cross section is described by its central filament $\boldsymbol{X}_0(s)$ and two vectors $\boldsymbol{n}(s)$ and $\boldsymbol{b}(s)$, which determine the spatial orientation of the coil cross section. In the far distance from the coil the magnetic field can be computed by Biot-Savart's law, however close to the coil higher order correction terms must be taken into account. A power series expansion allows to compute the field in a given precision. The expansion parameter is the width or height of the coil divided by the distance R_0 to the central filament. This procedure is of particlar importance in the boundary region of nested magnetic surfaces. Inside the coil the three-dimensional integration can be reduced to an one-dimensional one along the coil axis. Integration over the rectangular coil cross section leads to elementary functions. However, in

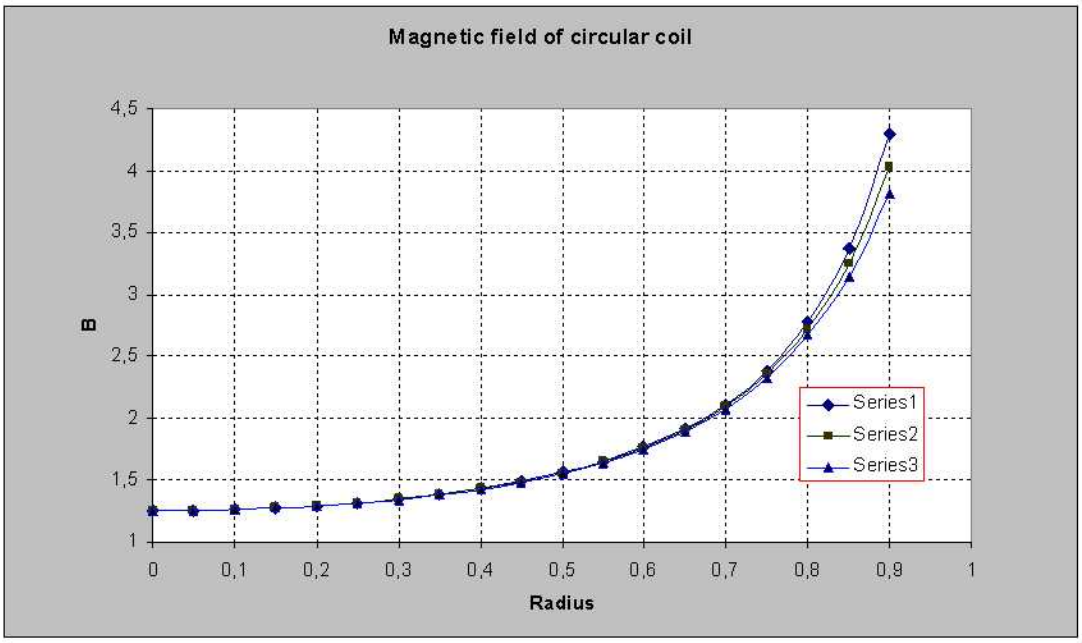

Figure 3: Magnetic field in the midplane of a circular coil

case of inhomogeneous current density and trapezoidal cross section, a reduction of the three-dimensional integration is not possible.

Numerical integration of the magnetic field in a circular coil demonstrates that the Biot-Savart approximation is not sufficient if a precision of 10^{-4} is required. In particular the boundary region of magnetic surfaces, where islands occur, a high precision $\delta B/B < 10^{-4}$ is needed since the size of islands strongly depends on resonant field components. Inside a coil such high precision of the computation is not needed. In order to reduce the maximum magnetic field at a fixed total coil current a trapezoidal cross section and inhomogeneous current density reducing the current density in the high-field region is helpful.

8 Appendix1, Biot-Savart approximation

8.1 Constant current density

At first, the current density is constant in a rectangular coil cross section. In order to find the approximation of the magnetic field in some distance from the coil we define the integrals

$$M_{i,k} = \int (y-y_0)^i (x-x_0)^k \, dxdy = \frac{1}{(i+1)(k+1)} \left[(h-y_0)^{i+1} - (-h-y_0)^{i+1}\right] \left[(b-x_0)^{k+1} - (-b-x_0)^{k+1}\right] \quad (69)$$

$M_{0,0} = 4hb$ is the area of the coil cross section. In order to find a recursive representation we define the functions p_i and q_i

$$p_i(x,y) = \frac{1}{i+1}(x-y)^{i+1} \quad , \quad q_i(x,y) = \frac{1}{i+1}(-1)^{i+1}(x+y)^{i+1} \quad (70)$$

which satisfy the recursive procedure

$$p_i(x,y) = \frac{i}{i+1}(x-y)p_{i-1}(x,y) \quad , \quad p_0 = (x-y) \tag{71}$$

$$q_i(x,y) = -\frac{i}{i+1}(x+y)q_{i-1}(x,y) \quad , \quad q_0 = -(x+y) \tag{72}$$

Using these functions we write

$$M_{i,k} = \left[p_i(h,y_0) - q_i(h,y_0)\right]\left[p_k(b,x_0) - q_k(b,x_0)\right] \tag{73}$$

The recursive relations for $p_i - q_i$ are

$$\begin{aligned} p_i - q_i &= \frac{i}{i+1}\left\{x(p_{i-1} - q_{i-1}) - y(p_{i-1} + q_{i-1})\right\} \\ p_i + q_i &= \frac{i}{i+1}\left\{x(p_{i-1} + q_{i-1}) - y(p_{i-1} - q_{i-1})\right\} \end{aligned} \tag{74}$$

The irst terms of M_{ik} are

$$\begin{aligned} M_{1,0} &= -y_0 M_{0,0} \quad , \quad M_{0,1} = -x_0 M_{0,0} \\ M_{2,0} &= \left(\frac{h^2}{3} + y_0^2\right) M_{0,0} \quad , \quad M_{0,2} = \left(\frac{b^2}{3} + x_0^2\right) M_{0,0} \\ M_{2,1} &= -x_0 M_{2,0} \quad , \quad M_{1,2} = -y_0 M_{0,2} \\ M_{2,2} &= \left(\frac{h^2}{3} + y_0^2\right)\left(\frac{b^2}{3} + x_0^2\right) M_{0,0} \quad , \quad M_{1,1} = x_0 y_0 M_{0,0} \\ M_{3,0} &= -y_0\left(y_0^2 + h^2\right) M_{0,0} \quad , \quad M_{0,3} = -x_0\left(x_0^2 + b^2\right) M_{0,0} \\ M_{3,1} &= -x_0 M_{3,0} \quad , \quad M_{1,3} = -y_0 M_{0,3} \end{aligned} \tag{75}$$

With the help of these functions and

$$q = (y-y_0)^2 + (x-x_0)^2 - r_0^2,\ r_0^2 = y_0^2 + x_0^2$$

we define

$$P_{i,k} = \int (y-y_0)^i (x-x_0)^k \, q \, dxdy = M_{i+2,k} + M_{i,k+2} - r_0^2 M_{i,k} \tag{76}$$

and together with

$$q^2 = (y-y_0)^4 + (x-x_0)^4 + 2(y-y_0)^2(x-x_0)^2 - 2r_0^2(y-y_0)^2 - 2r_0^2(x-x_0)^2 + r_0^4$$

we get

$$\begin{aligned} Q_{i,k} &= \int (y-y_0)^i (x-x_0)^k \, q^2 \, dxdy = \\ & M_{i+4,k} + M_{i,k+4} + 2M_{i+2,k+2} - 2r_0^2 M_{i+2,k} - 2r_0^2 M_{i,k+2} + r_0^4 M_{i,k} \end{aligned} \tag{77}$$

The power series expansion of $1/N$ yields

$$
\begin{aligned}
F_1 &= \frac{1}{R_0}\int\left[1-\frac{1}{2}\frac{q}{R_0^2}+\frac{3}{8}\frac{q^2}{R_0^4}-...\right]dydx \\
&= \frac{1}{R_0}\left[M_{0,0}-\frac{1}{2}\frac{P_{0,0}}{R_0^2}+\frac{3}{8}\frac{Q_{0,0}}{R_0^4}-...\right] \\
F_2 &= \frac{1}{R_0}\int(y-y_0)\left[1-\frac{1}{2}\frac{q}{R_0^2}+\frac{3}{8}\frac{q^2}{R_0^4}-...\right]dydx \\
&= \frac{1}{R_0}\left[M_{1,0}-\frac{1}{2}\frac{P_{1,0}}{R_0^2}+\frac{3}{8}\frac{Q_{1,0}}{R_0^4}-...\right] \\
F_3 &= \frac{1}{R_0}\int(x-x_0)\left[1-\frac{1}{2}\frac{q}{R_0^2}+\frac{3}{8}\frac{q^2}{R_0^4}-...\right]dydx \\
&= \frac{1}{R_0}\left[M_{0,1}-\frac{1}{2}\frac{P_{0,1}}{R_0^2}+\frac{3}{8}\frac{Q_{0,1}}{R_0^4}-...\right] \\
F_4 &= \frac{1}{R_0^3}\int(y-y_0)\left[1-\frac{3}{2}\frac{q}{R_0^2}+\frac{15}{8}\frac{q^2}{R_0^4}-...\right]dydx \\
&= \frac{1}{R_0^3}\left[M_{1,0}-\frac{3}{2}\frac{P_{1,0}}{R_0^2}+\frac{15}{8}\frac{Q_{1,0}}{R_0^4}-...\right] \\
F_5 &= \frac{1}{R_0^3}\int(x-x_0)\left[1-\frac{3}{2}\frac{q}{R_0^2}+\frac{15}{8}\frac{q^2}{R_0^4}-...\right]dydx \\
&= \frac{1}{R_0^3}\left[M_{0,1}-\frac{3}{2}\frac{P_{0,1}}{R_0^2}+\frac{15}{8}\frac{Q_{0,1}}{R_0^4}-...\right] \\
F_6 &= \frac{1}{R_0^3}\int(y-y_0)(x-x_0)\left[1-\frac{3}{2}\frac{q}{R_0^2}+\frac{15}{8}\frac{q^2}{R_0^4}-...\right]dydx \\
&= \frac{1}{R_0^3}\left[M_{1,1}-\frac{3}{2}\frac{P_{1,1}}{R_0^2}+\frac{15}{8}\frac{Q_{1,1}}{R_0^4}-...\right] \\
F_7 &= \frac{1}{R_0^3}\int(y-y_0)^2\left[1-\frac{3}{2}\frac{q}{R_0^2}+\frac{15}{8}\frac{q^2}{R_0^4}-...\right] \\
&= \frac{1}{R_0^3}\left[M_{2,0}-\frac{3}{2}\frac{P_{2,0}}{R_0^2}+\frac{15}{8}\frac{Q_{2,0}}{R_0^4}-...\right] \\
F_8 &= \frac{1}{R_0^3}\int(x-x_0)^2\left[1-\frac{3}{2}\frac{q}{R_0^2}+\frac{15}{8}\frac{q^2}{R_0^4}-...\right] \\
&= \frac{1}{R_0^3}\left[M_{0,2}-\frac{3}{2}\frac{P_{0,2}}{R_0^2}+\frac{15}{8}\frac{Q_{0,2}}{R_0^4}-...\right] \qquad (78)
\end{aligned}
$$

8.2 Inhomogeneous current density

In case of trapezoidal coil cross section the current density is a function of the vertical coordinate y and the functions M_{ik} must be defined as

$$
\begin{aligned}
M_{i,k} &= \int j(y)(y-y_0)^i(x-x_0)^k\,dxdy = \\
&\frac{1}{k+1}\int_{-h}^{h} j(y)(y-y_0)^i\left[(b(y)-x_0)^{k+1}-(-b(y)-x_0)^{k+1}\right]dy \qquad (79)
\end{aligned}
$$

Integration over y is left to numerical methods. The other quantities are

$$P_{i,k} = \int j(y)(y-y_0)^i (x-x_0)^k \, q \, dxdy = M_{i+2,k} + M_{i,k+2} - r_0^2 M_{i,k} \tag{80}$$

and

$$\begin{aligned} Q_{i,k} &= \int j(y)(y-y_0)^i (x-x_0)^k \, q^2 \, dxdy = \\ & M_{i+4,k} + M_{i,k+4} + 2M_{i+2,k+2} - 2r_0^2 M_{i+2,k} - 2r_0^2 M_{i,k+2} + r_0^4 M_{i,k} \end{aligned} \tag{81}$$

where the functions M_{ik} are given in 79. The rest of the computation follows the same line as shown in the previous section.

9 Appendix 2, analytic solution

9.1 Constant current density

In section 4 we defined the functions $F_1, ..., F_8$. These function can expressed in terms of elementary functions if the current density is constant. In the following some functions will be given which are needed in computing the $F_1, .., F_8$.

$$F(x, A, B) := \int \frac{dx}{\sqrt{x^2 + A^2 + B^2}} = \ln\left(x + \sqrt{x^2 + A^2 + B^2}\right) + C \tag{82}$$

The function $F(x, 0, B)$ has a logarithmic singularity in B for any negative x-value.

$$G(x, A, B) := \int \sqrt{x^2 + A^2 + B^2}\, dx = \frac{x}{2}\sqrt{x^2 + A^2 + B^2} + \frac{A^2 + B^2}{2} F(x, A, B) + C \tag{83}$$

$$H(x, A, B) := \int \frac{dx}{(\sqrt{x^2 + A^2 + B^2})^3} = \frac{x}{(A^2 + B^2)\sqrt{x^2 + A^2 + B^2}} + C \tag{84}$$

$$\begin{aligned} I(A, B, x): &= \int \ln\left(A + \sqrt{x^2 + A^2 + B^2}\right) dx = \int F(A, B, x)\, dx \\ &= xF(A, B, x) - x + AF(x, B, A) \\ &- \sqrt{B^2} \arctan\left(\frac{B^2 + A(A + \sqrt{x^2 + A^2 + B^2}}{\sqrt{B^2}x}\right) + C \end{aligned} \tag{85}$$

Using these integrals we get

$$\begin{aligned} F_1 &= \int \frac{dxdy}{\sqrt{s_0^2 + (x - x_0)^2 + (y - y_0)^2}} \\ &= \int_{-h}^{h} \left[F(b - x_0, y - y_0, s_0) - F(-b - x_0, y - y_0, s_0)\right] dy \end{aligned} \tag{86}$$

This integral exists and is finite if for any finite $s_0 \neq 0$. The function $F(b - x_0, y - y_0, s_0)$ has a logarithmic singularity at $y = y_0, s_0 = 0$. However, since a logarithmic singularity is integrable, the integral F_1 is finite for any point inside and outside the cross section. With the help of eq. (85) the integration over y yields

$$\begin{aligned} F_1(h, b, x_0, y_0, s_0) &= I(h - y_0, b - x_0, s_0) - I(h - y_0, -b - x_0, s_0) \\ &- I(-h - y_0, b - x_0, s_0) + I(-h - y_0, -b - x_0, s_0) \end{aligned} \tag{87}$$

Next, we compute F_2 and F_3.

$$\begin{aligned} F_2 &= \int \frac{y-y_0}{N(\boldsymbol{X},s,y,x)}\,dydx = \int \frac{\partial}{\partial y} N(\boldsymbol{X},s,y,x)\,dydx \\ F_3 &= \int \frac{x-x_0}{N(\boldsymbol{X},s,y,x)}\,dydx = \int \frac{\partial}{\partial x} N(\boldsymbol{X},s,y,x)\,dydx \end{aligned} \tag{88}$$

With help of eq.(83 we get

$$\int N\,dx = G(x-x_0,y-y_0,s_0) \quad ; \quad \int N\,dy = G(y-y_0,x-x_0,s_0) \tag{89}$$

and

$$\begin{aligned} F_2 &= G(b-x_0,h-y_0,s_0) + G(-b-x_0,h+y_0,s_0) \\ &- G(b-x_0,h+y_0,s_0) - G(-b-x_0,h-y_0,s_0) \end{aligned} \tag{90}$$

The function F_3 is

$$\begin{aligned} F_3 &= G(h-y_0,b-x_0,s_0) + G(-h-y_0,b+x_0,s_0) \\ &- G(h-y_0,b+x_0,s_0) - G(-h-y_0,b-x_0,s_0) \end{aligned} \tag{91}$$

The structure of the functions $F_4,...,F_8$ is as follows

$$F_l = \int \frac{(y-y_0)^i (x-x_0)^k}{N^3(\boldsymbol{X},s,y,x)}\,dydx \quad ; \quad i,k \leq 2 \tag{92}$$

With the help

$$\frac{(y-y_0)}{N^3(\boldsymbol{X},s,y,x)} = -\frac{\partial}{\partial y}\frac{1}{N} \quad ; \quad \frac{(x-x_0)}{N^3(\boldsymbol{X},s,y,x)} = -\frac{\partial}{\partial x}\frac{1}{N} \tag{93}$$

we get

$$\begin{aligned} F_4 = -\int_{-b}^{b} \left[\frac{1}{N}\right]_{-h}^{h} dx &= -F(b-x_0,h-y_0,s_0) - F(-b-x_0,-h-y_0,s_0) \\ &+ F(-b-x_0,h-y_0,s_0) + F(b-x_0,-h-y_0,s_0) \end{aligned} \tag{94}$$

and

$$\begin{aligned} F_5 = -\int_{-h}^{h} \left[\frac{1}{N}\right]_{-b}^{b} dy &= -F(h-y_0,b-x_0,s_0) - F(-h-y_0,-b-x_0,s_0) \\ &+ F(h-y_0,-b-x_0,s_0) + F(-h-y_0,b-x_0,s_0) \end{aligned} \tag{95}$$

The function $F(x,y,s)$ is defined in eq.(82). Because of

$$\frac{(y-y_0)(x-x_0)}{N^3} = -\frac{\partial^2 N}{\partial x \partial y} \tag{96}$$

the function F_6 is

$$F_6 = -N(h-y_0,b-x_0) - N(-h-y_0,-b-x_0) + N(h-y_0,-b-x_0) + N(-h-y_0,b-x_0) \tag{97}$$

Partial integration yields

$$\begin{aligned} F_7 &= -\int \frac{\partial}{\partial y}\frac{(y-y_0)}{N}\,dxdy + \int \frac{1}{N}\,dxdy \\ &= -\int \frac{\partial}{\partial y}\left((y-y_0)\int_{-b}^{b}\frac{1}{N}\,dx\right)dy + \int \frac{1}{N}\,dxdy \\ &= -\int \frac{\partial}{\partial y}\left[(y-y_0)\left(F(b-x_0,y-y_0,s_0)-F(-b-x_0,y-y_0,s_0)\right)\right] \\ &+ \int \frac{1}{N}\,dxdy \end{aligned} \tag{98}$$

The last term is equal to F_1 and the result is

$$\begin{aligned} F_7 &= -(h-y_0)\left(F(b-x_0,h-y_0,s_0)-F(-b-x_0,h-y_0,s_0)\right) \\ &+ (-h-y_0)\left(F(b-x_0,-h-y_0,s_0)-F(-b-x_0,-h-y_0,s_0)\right)+F_1 \end{aligned} \tag{99}$$

$$\begin{aligned} F_8 &= -(b-x_0)\left(F(h-y_0,b-x_0,s_0)-F(-h-y_0,b-x_0,s_0)\right) \\ &+ (-b-x_0)\left(F(h-y_0,-b-x_0,s_0)-F(-h-y_0,-b-x_0,s_0)\right)+F_1 \end{aligned} \tag{100}$$

9.2 Straight rectangular segment

The magnetic field of a straight segment is (see eq.44)

$$\boldsymbol{B}(\boldsymbol{X}) = \frac{\mu_0}{4\pi}\oint\left[F_4\boldsymbol{b}-F_5\boldsymbol{n}\right]ds \tag{101}$$

The two vectors $\boldsymbol{b},\boldsymbol{n}$ are independent of s. In computing the integration of F_4, F_5 we note that the components x_0, y_0 do not depend on s and we can identify the component s_0 with s. This leads to the following integral (see eq. (85))

$$\int \ln(X+\sqrt{s^2+X^2+Y^2})\,ds = \int F(X, s^2+X^2+Y^2)\,ds = I(X,Y,s) \tag{102}$$

Inserting these results into 101 yields

$$\begin{aligned} \int F_4\,ds &= -\int\left\{F(b-x_0,h-y_0)+F(-b-x_0,-h-y_0)\right\}ds \\ &+ \int\left\{F(-b-x_0,h-y_0)+F(b-x_0,-h-y_0)\right\}ds \\ &= -I(b-x_0,h-y_0,s)-I(-b-x_0,-h-y_0,s) \\ &+ I(-b-x_0,h-y_0,s)+I(b-x_0,-h-y_0,s) \end{aligned} \tag{103}$$

and

$$\begin{aligned} \int F_5\,ds &= \int\left\{-F(h-y_0,b-x_0)-F(-h-y_0,-b-x_0)\right\}ds \\ &+ \int\left\{F(h-y_0,-b-x_0)+F(-h-y_0,b-x_0)\right\}ds \\ &= -I(h-y_0,b-x_0,s)-I(-h-y_0,-b-x_0,s) \\ &+ I(h-y_0,-b-x_0,s)+I(-h-y_0,b-x_0,s) \end{aligned} \tag{104}$$

The function I is given in 85. Because of the alternating sign on the right hand side the linear term in s does not contribute. The results coincide with those used in the EFFI-code [2].

9.3 Inhomogeneous current density

We consider a trapezoidal coil cross section and a current density which depends on the y-coordinate. The width of the winding pack is $b(y)$. The functions $F_1, ..., F_3$ are

$$\begin{aligned} F_1 &= \int_{-h}^{h} j(y) \int_{-b(y)}^{b(y)} \frac{dxdy}{N} \\ F_2 &= \int_{-h}^{h} j(y)(y-y_0) \int_{-b(y)}^{b(y)} \frac{dxdy}{N} \\ F_3 &= \int_{-h}^{h} j(y) \int_{-b(y)}^{b(y)} (x-x_0) \frac{dxdy}{N} \end{aligned} \tag{105}$$

The integration over x yields

$$\begin{aligned} F_1 &= \int_{-h}^{h} j(y) \left[F(b(y)-x_0, y-y_0) - F(-b(y)-x_0, y-y_0)\right] dy \\ F_2 &= \int_{-h}^{h} j(y)(y-y_0) \left[F(b(y)-x_0, y-y_0) - F(-b(y)-x_0, y-y_0)\right] dy \end{aligned} \tag{106}$$

and

$$F_3 = \int_{-h}^{h} j(y) \left[N(b(y)-x_0, y-y_0) - N(-b(y)-x_0, y-y_0)\right] dy \tag{107}$$

We define the function

$$H(a^2, z) = \int \frac{dz}{(a^2+z^2)^{3/2}} = \frac{z}{a^2(a^2+z^2)^{1/2}} \tag{108}$$

and write F_4 as follows

$$F_4 = \int_{-h}^{h} j(y)(y-y_0) \left[H(s_0^2 + (y-y_0)^2, b(y)-x_0) - H(s_0^2 + (y-y_0)^2, -b(y)-x_0)\right] dy \tag{109}$$

or

$$F_4 = \int_{-h}^{h} \frac{j(y)(y-y_0)}{s_0^2 + (y-y_0)^2} \left[\frac{1}{\sqrt{s_0^2 + (y-y_0)^2 + (b-x_0)^2}} - \frac{1}{\sqrt{(s_0^2 + (y-y_0)^2 + (b+x_0)^2}}\right] dy \tag{110}$$

$b = b(y)$. The function F_5 and F_6 are

$$F_5 = \int_{-h}^{h} j(y) \left[\frac{1}{\sqrt{s_0^2 + (y-y_0)^2 + (b+x_0)^2}} - \frac{1}{\sqrt{(s_0^2 + (y-y_0)^2 + (b-x_0)^2}}\right] dy \tag{111}$$

$$F_6 = \int_{-h}^{h} j(y) \left[\frac{y-y_0}{\sqrt{(s_0^2 + (y-y_0)^2 + (b+x_0)^2}} - \frac{y-y_0}{\sqrt{(s_0^2 + (y-y_0)^2 + (b-x_0)^2}}\right] dy \tag{112}$$

F_7 is

$$F_7 = \int_{-h}^{h} j(y)(y-y_0)^2 \left[H(s_0^2 + (y-y_0)^2, b(y)-x_0) - H(s_0^2 + (y-y_0)^2, -b(y)-x_0)\right] dy \tag{113}$$

or in explicit form

$$F_7 = \int_{-h}^{h} \frac{j(y)(y-y_0)^2}{s_0^2+(y-y_0)^2} \left[\frac{1}{\sqrt{s_0^2+(y-y_0)^2+(b-x_0)^2}} - \frac{1}{\sqrt{(s_0^2+(y-y_0)^2+(b+x_0)^2}} \right] dy \tag{114}$$

For computing F_8 we refer to

$$\frac{(x-x_0)^2}{N^3} = -\frac{\partial}{\partial x}\left(\frac{(x-x_0)}{N}\right) + \frac{1}{N} \tag{115}$$

and find after partial integration

$$F_8 = F_1 - \int_{-h}^{h} \left[\frac{j(y)(b-x_0)}{\sqrt{(s_0^2+(y-y_0)^2+(b-x_0)^2}} + \frac{j(y)(b+x_0)}{\sqrt{(s_0^2+(y-y_0)^2+(b+x_0)^2}} \right] dy \tag{116}$$

References

[1] H. Wobig and S. Rehker, *A Stellarator Coil System without Helical Windings*, Proc. 7th Symp. on Fusion Technology, Grenoble, France, 333-343 (October 24-27, 1972).

[2] S.J.Sackett, LLNL report UCRL-52402, 1978

[3] Urankar L. *Vector potential and magnetic field of current-carrying finite arc segment in analytical form* Part I: filament approximation. IEEE Transactions on Magnetics 1980; 16:12831288.

[4] Urankar L. *Vector potential and magnetic field of current-carrying finite arc segment in analytical form* Part II: thin sheet approximation. IEEE Transactions on Magnetics 1982; 18:911917.

[5] Urankar L., *Vector potential and magnetic field of current-carrying finite arc segment in analytical form* Part III: exact computation for rectangular cross section. IEEE Transactions on Magnetics 1982; 18:18601867.

[6] Urankar L., *Vector potential and magnetic field of current-carrying finite arc segment in analytical form* Part IV: general three-dimensional current density. IEEE Transactions on Magnetics 1984; 20:21452150.

[7] M. Fontana, *Integration methods for the calculation of the magnetic field due to coils*, Preprint 2001-07, Chalmers University of Technology, Gteborg, Sweden 2001

[8] Slobodan I. Babic and Cevdet Akyelz, *An improvement in the calculation of the magnetic field for an arbitrary geometry coil with rectangular cross section*, Int. J. Numer. Model. 2005; 18:493504

[9] Donald R. Wilton, senior member, IEEE, S. M. Rao, Allen W. Glisson, member, IEEE, Daniel H. Schaubert, senior member, IEEE, 0. M. Al-Bundak and Chalmers W. Buttler, Fellow, IEEE, *Potential Integrals for Uniform and Linear Source Distribution on Polygonal and Polyhedral Domains*, IEEE Transactions on antennas and propagation, VOL. AP-32, NO. 3, March 1984